2024 IEEE International Symposium on Electromagnetic Compatibility, Signal & Power Integrity (EMC+SIPI) | 979-8-3503-6039-4/24/$31.00 ©2024 IEEE | DOI: 10.1109/EMCSIPI49824.2024.10705508

On Comparing Interference Impacts

Aric Sanders[†], Michelle Pirrone[†,*], M. Keith Forsyth[†], Adam Wunderlich[†]
[†]*Communications Technology Laboratory*, *National Institute of Standards and Technology, Boulder, Colorado USA*
[*]*Department of Electrical, Computer, and Energy Engineering*, *University of Colorado Boulder*, *Boulder, Colorado USA*
{aric.sanders,michelle.pirrone, keith.forsyth, adam.wunderlich}@nist.gov

***Abstract*—Interference between communication systems is a critical issue that can impact performance and operability of devices. A wide range of methods and testbeds have been developed to study susceptibility to interference, and each of these testbeds and their experimental test schedules can have different factors and responses. Although there is a variety in testbed design and measurement, it is common to choose a response that is assumed to vary with signal-to-noise ratio. A fundamental issue in any interference study of this type is the assignment of the power of the interference signal in a way that represents the desired environmental situation. This can be a challenging task for signals with disparate time, frequency and power dynamics. In particular, whether to assign a maximum (peak power) or a time averaged power becomes ambiguous for inter-interference signal comparisons. To address this problem we propose a quantitative scale based on the impact on the receiver of interest. We demonstrate how to form an interference signal agnostic scale and apply that scale for different interference situations. This scale, impact equivalent power ratio, can be transformed into an impact equivalent power with knowledge of the effective noise figure of the system under test.**

I. Introduction

The continuous, rapid expansion of communication devices in an increasingly congested frequency spectrum has focused attention on the need to characterize and understand interference between these devices. For example, in the highly desirable mid-band spectrum ($1\ GHz - 6\ GHz$), there are multiple technologies that coexist at the same frequency and many others that share adjacent bands. Specifically in the 2.4 GHz ISM band, technologies such as Zigbee, WiFi and Bluetooth operate simultaneously on the same frequencies [1], similar usage situations occur at $5\ GHz$ [2], and $6\ GHz$ [3]. Some frequency bands now even allow shared use between mission-critical military assets and consumer products, such as the Citizens Broadband Radio Service [4]. In addition, even more incumbent users have new licensees in adjacent frequency bands, such as Long Term Evolution (LTE) adjacent to aeronautical mobile telemetry (AMT) [5] and 5G adjacent to radar altimeter bands [6]. Each of these situations involves interactions between systems and a need to compare the impact of interference on victim systems.

To facilitate comparison of interference impacts across different victim systems and environments, we propose a relative measure, called the impact equivalent power ratio (IEPR), defined as the excess signal power required to equalize a system KPI to its value in the absence of an interfering signal. Specifically, suppose that the KPI is some function of SNR, i.e. KPI(S/N), where S and N denote power for the signal and noise, respectively. Moreover, we assume that for a given level of interference, the KPI takes a value that is equivalent to a value without interference, i.e., KPI(S/N) = KPI(S'/N'), where KPI(S/N) and KPI(S'/N') denote the responses of the system without and with interference, respectively. Here we have intentionally replaced the signal-to-noise plus interference ratio with a signal-to-noise ratio equivalent. Since $S/N = S'/N'$ implies $S'/S = N'/N$, it follows that IEPR $= S'/S$ is equal to the ratio of excess noise, which reflects the interference impact.

In practice, the IEPR value for realistic signals can be extremely difficult to predict, requiring foreknowledge about the communications protocol, RF-frontend frequency response, and complete knowledge of the transmitted and interference signal. However, the Impact Equivalent Power Ratio (IEPR) value can be measured experimentally in relation to a control or reference response for the system without the interfering signal of interest present. With this control response, other impacts can be compared by finding the value of the received signal power where the KPI is equal. Figure 1 depicts a notional situation in which a KPI for a victim receiver is measured in three distinct conditions: with no interference, and with interference from two different sources. Using the KPI without interference as a control, the two conditions with signals can be recast in terms of an IEPR whose magnitude is equal to the ratio of signal power in the control condition and the two interference conditions. Note that IEPR does not depend on specifics of the interference signal, only its quantifiable impact on the system under test (SUT). Thus, IEPR characterizes the impact of interfering signals of any type on different SUTs in a universal way.

II. Experimental Examples

In this section, test results from multiple testbeds, in different modes of operation, are presented to show the utility of IEPR. Details on the design and verification of these testbeds are covered in detail elsewhere [5], [7]. The key assumptions required for the construction of IEPR are:

- The test in consideration depends on a key performance indicator (KPI).
- This key performance indicator depends on the SNR of the SUT.
- The test can be performed in the presence and absence of an interference signal of interest.

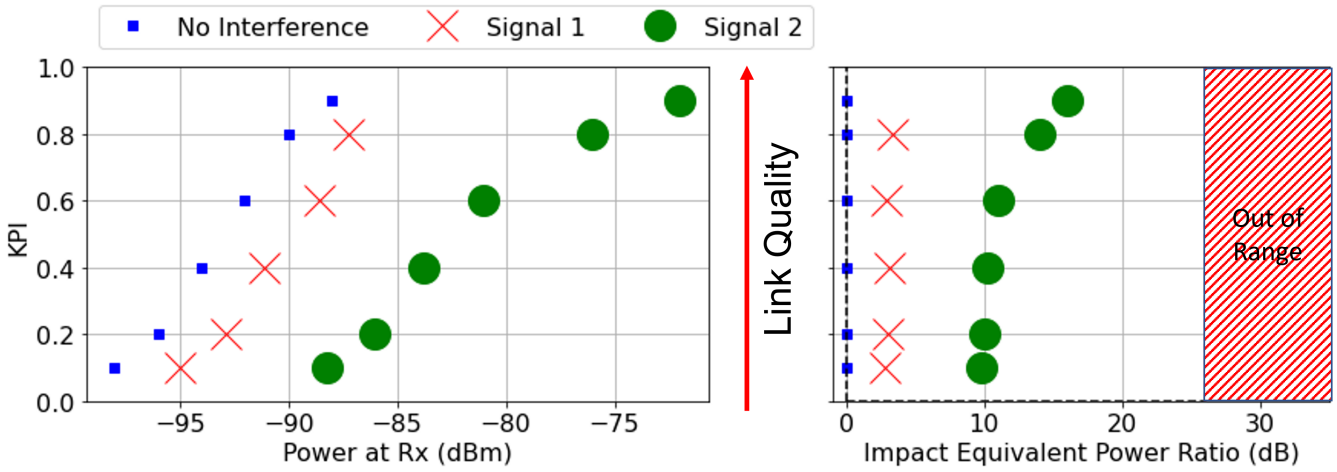

Figure 1. Schematic of scale construction. Left shows an arbitrary KPI that scales with SNR and right shows a normalized scale using the lack of an interference signal as a control.

- The power of the communications signal at the receiver is known.

If these criteria are met, then the IEPR is simply the difference of the signal power, in log units, for the interference-present and interference-absent cases when the KPI is equal.

Below, we use the following conventions to denote injected signal power levels. For noise signals, we quantify their strength in units of power spectral density ($\frac{dBm}{Hz}$) whereas for other types of co-channel (CC) and adjacent-band (AB) interference signals we use the root mean squared (RMS) power at the plane of the receiver.

A. LTE Effects on AMT

In this example, we explore data from a study examining the effects of adjacent band interference on AMT [5]. We begin with a side-experiment, labeled Side Experiment C in the original study [5, Appendix C], that examined the impacts of CC excess additive white Gaussian noise (AWGN) on the receiver. In this side-experiment, different modulation schemes and data rates were tested at three excess noise levels. In Fig. 2, we show results for the following modulation schemes at a bitrate of 5 megabits per second (Mbps): pulse-code-modulation (PCM)/frequency-modulation (FM), advanced ranging telemetry continuous phase modulation (ARTM CPM), and shaped-offset quadrature phase-shift keying (SOQPSK). The no-excess-noise condition is labeled control, and in addition to the CC AWGN impacts, we plot the response for a single AB LTE interference signal. For more details on the signal properties see [5, Tables 3.4, 3.5, A.6] and for a description of the LTE recording methods see [8].

In Fig. 2, in the upper row, the base ten logarithm of bit error rate (BER) is plotted with respect to received signal power. The choice of KPI means the more negative $Log_{10}(\text{BER})$ is, the higher quality the link. In each condition, the effect of introducing AWGN to the channel is to simply increase the power required to obtain the same BER. In the lower row of Fig. 2, we show the calculated IEPR; see Sec. III for calculation methods. Interestingly, the IEPR of signals from recorded LTE introduced as an AB interference do not always show noise-like behavior. Here, the IEPR of the LTE takes significantly different values based on the link condition, in this case varying over $5\ dB$ for different KPI values.

B. Co-Channel Interference Impact on Point-to-Point Links

As a second example of the utility of IEPR, we show the impact of interference on a microwave point-to-point link. The experimental setup is documented in [7], with the following differences:

- The ettus x410 SDR is replaced by a Rhode and Schwartz Vector Signal Generator [1].
- The iperf3 network throughput tool is replaced by a proprietary diagnostic tool.
- An amplified noise diode is used as the source of white-noise.

Unlike the previous example, the KPI of interest is data throughput. The data throughput is measured every second for the SUT over an interval of 300 s. The last five throughput measurements are averaged to insure a stable, steady-state result. In Fig. 3, results for five total test conditions are depicted: the control condition with no interference, excess injected noise from a noise diode, denoted ND, at two power levels, and two powers of a co-channel LTE Signal. The LTE signal is similar to that used in Sec. II-A, introduced as CC interference. The results in Fig. 3 have been limited to throughput values between $60\ Mbps$ and $15\ Mbps$ to avoid extended areas in which the rate of change is zero; see implementation details in the next section.

[1]Certain commercial products or company names are identified here to describe our study adequately. Such identification is not intended to imply recommendation or endorsement by the National Institute of Standards and Technology, nor is it intended to imply that the products or names identified are necessarily the best available for the purpose.

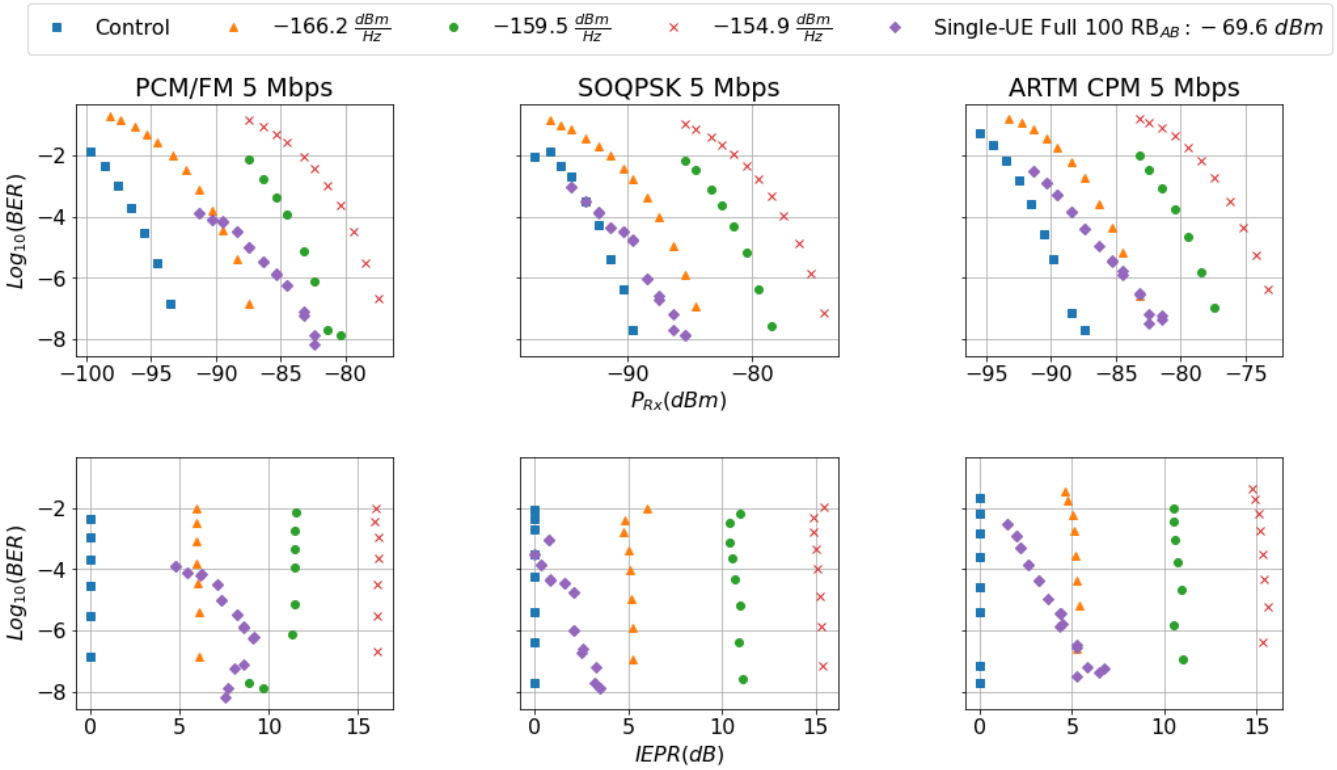

Figure 2. Comparison of the base ten logarithm of bit error rate (BER) versus signal power at the receiver for an AMT communication link in the presence of of different co-channel white noise interference and adjacent-channel LTE interference. Derived from results in Young et al. [5].

Examining Fig. 3, we observe that impact of the noise diode is similar qualitatively to the AWGN injected in the first example. In particular, the IEPR does not change as the link is degraded. This is contrasted by the CC LTE interference that has a larger impact at higher data throughputs, or higher link quality.

III. Methods of Calculation, Uncertainty and Limitations

To calculate IEPR from discrete KPI observations, there are two general approaches. The first, termed inverse regression, obtains a continuous KPI response curve as a function of RX power for the control (no interference) condition via a forward regression and then inverts the function to obtain RX power as a function of the KPI. The second approach, termed reverse regression, directly fits the RX power as a function of the KPI value [9], [10] for the control (no interference) condition. Here, we choose the second approach because the uncertainties in the RX power exceed those in the KPI. The IEPR is the value of the reverse regression evaluated at each discrete KPI observation under the interference condition.

In Fig. 4, we compare the sensitivity of IEPR calculated with various reverse regression schemes. Namely, for the point-to-point microwave link detailed in Sec. II-B, we measured the throughput over a range of noise conditions achieved with a noise diode. First, the control response was measured by sweeping signal power in 1 dB steps in the absence of excess noise. Next, additive noise was injected via noise diode and programmable attenuator such that at the victim RX input the excess noise power ranged from -169.2 ± 0.9 $\frac{dBm}{Hz}$ to -151.2 ± 0.9 $\frac{dBm}{Hz}$ in 1 dB steps.

Here, we compare three types of regression, locally estimated scatterplot smoothing (LOESS) as implemented by [11], a 1-d linear interpolation, and a smoothing spline [12]. Fig. 4 (Middle) shows the resulting residuals, which demonstrate that the choice of regression only has a small impact in this case.

The resulting IEPR versus noise power curve in Fig. 4 (Top, right axis label) shows that for white-noise the IEPR scale is linear. In this case, IEPR acts as a power detector, where the scale can be decomposed as $N_0 = N_{\text{th}} + \text{NF}_{\text{effective}}$, with N_{th} and $NF_{\text{effective}}$ denoting the thermal noise level and effective noise figure, expressed in decibels. If the thermal noise floor and the effective noise figure are known, then we can define a related metric, the Impact Equivalent Power (IEP) as the IEPR + N_0 in decibels; see Fig. 4 (Top, left axis label). The IEP scale quantifies interference impact in absolute power units.

To determine the Effective Noise Figure ($\text{NF}_{\text{Effective}}$) of the SUT, we applied a method similar to the one outlined in [13]. The uncertainty of the $\text{NF}_{\text{Effective}}$ was determined using a Monte Carlo approach, based on the power uncertainty and the uncertainty in the attenuator settings, yielding an estimate of $\text{NF}_{\text{Effective}} = 6.4 \pm 1.1\ dB$, leading to an estimated system noise of $N_0 = -167.6 \pm 1.1$ $\frac{dBm}{Hz}$.

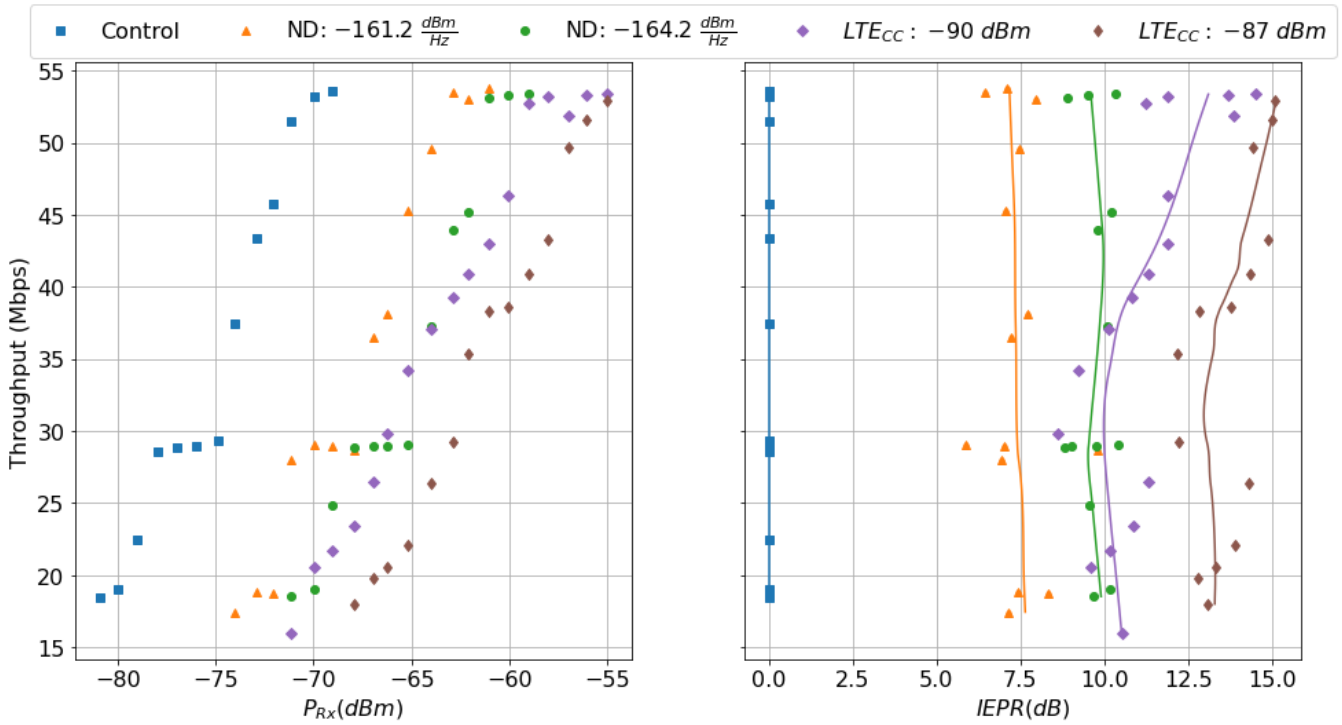

Figure 3. Comparison of data throughput in the presence of co-channel interference for a microwave point-to-point link. Above, Control denotes no interference, ND denotes noise injected from a noise diode, and LTE_{CC} denoted co-channel LTE. To aid interpretation, the plot on the right includes fitted trend lines.

A conservative estimate of the total uncertainty is given in Table I, where three principal uncertainties are considered; the uncertainty from choice of regression method ($\Delta_{Regression}$), the uncertainty from the internal variation of the IEPR as assessed using the inter-quartile range (Δ_{IQR}), and the uncertainty in N_0 (σ_{power}) determined from Monte-Carlo methods. The resultant total expanded uncertainty in the IEP is ± 3.2 $\frac{dBm}{Hz}$.

Table I
UNCERTAINTY OF IEP (IN DECIBELS)

$\Delta_{Regression}$	Δ_{IQR}	σ_{power}	$2 * \sigma_{total}$
0.09	1.2	1.1	3.2

A practical issue concerning the IEPR estimation procedure occurs when the reverse regression curve is not well-defined. For example, in Fig. 3 at throughput values around 30 Mbps, the KPI has a small rate of change giving the resultant IEPRs estimate much higher uncertainty.

In addition, the range of the IEPR scale is limited to the interval between the first measurable impact of a interference signal to the point at which the communication link is broken by that signal. For example, if the victim SUT employs an adaptive modulation scheme with a 256-QAM maximum modulation order, the total range may be 26 dB whereas an SUT capable of higher-order modulations, e.g., 1024-QAM, may have a total range of 35 dB.

IV. CONCLUSION

In conclusion, we have presented IEPR as a practical way to determine and compare the impact of interference signals on a SUT. In addition, we have presented IEP as a method of comparing interference impacts between SUTs.

As an example, the IEPR was used to quantify the impact of CC and AB interference signals on AMT. In addition, the impact on point-to-pont microwave links from CC signals was demonstrated. Finally, the IEPR scale was transformed into a IEP with knowledge of the system $\text{NF}_{\text{Effective}}$ and ambient thermal noise.

ACKNOWLEDGMENT

The authors wish to thank to Dr. Daniel Kuester for valuable input. This work was supported by the National Institute of Standards and Technology. MP was supported by the National Defense Science and Graduate Fellowship Program (NDSEG) through the University of Colorado Boulder.

REFERENCES

[1] R. G. Garroppo, L. Gazzarrini, S. Giordano, and L. Tavanti, "Experimental assessment of the coexistence of wi-fi, zigbee, and bluetooth devices," in *2011 IEEE International Symposium on a World of Wireless, Mobile and Multimedia Networks*, 2011, pp. 1–9.

[2] G. Naik, J. Liu, and J.-M. J. Park, "Coexistence of wireless technologies in the 5 ghz bands: A survey of existing solutions and a roadmap for future research," *IEEE Communications Surveys & Tutorials*, vol. 20, no. 3, pp. 1777–1798, 2018.

[3] G. Naik and J.-M. J. Park, "Coexistence of wi-fi 6e and 5g nr-u: Can we do better in the 6 ghz bands?" in *IEEE INFOCOM 2021 - IEEE Conference on Computer Communications*, 2021, pp. 1–10.

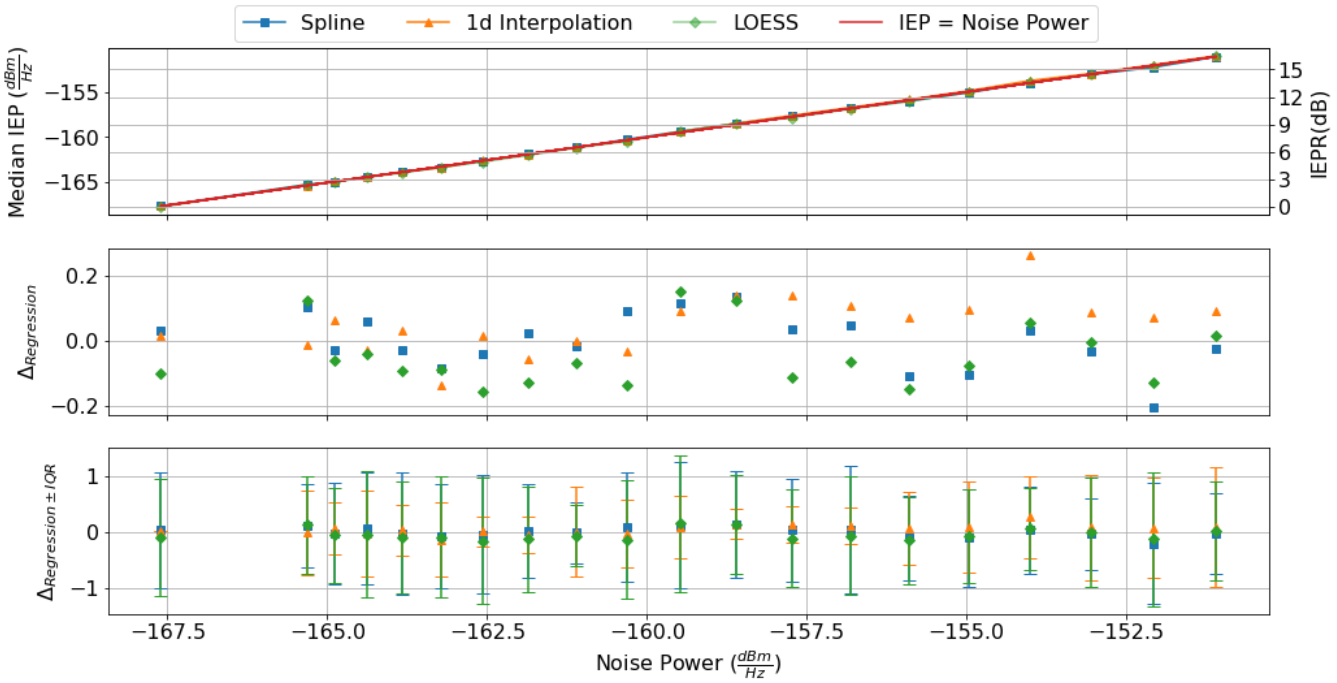

Figure 4. Comparison of various reverse regression schemes for IEPR estimation. Top: Estimated IEPR and IEP plotted versus total noise power at the RX. Middle: Residuals (in dB) for each regression method. Bottom: Uncertainty intervals (in dB) for the regression residuals expressed in terms of inter-quartile ranges obtained via Monte-Carlo error propagation.

[4] Federal Communication Commission, "3.5 GHz Band Overview," 2023. [Online]. Available: https://www.fcc.gov/wireless/bureau-divisions/mobility-division/35-ghz-band/35-ghz-band-overview

[5] W. Young, D. McGillivray, A. Wunderlich, M. Krangle, J. Sklar, A. Sanders *et al.*, "AWS-3 LTE Impacts on Aeronautical Mobile Telemetry," National Institute of Standards and Technology, Gaithersburg, MD, Tech. Rep. Technical Note 2140, Feb 2021.

[6] F. H. Sanders, K. R. Calahan, G. A. Sanders, and S. Tran, "Measurements of 5G New Radio Spectral and Spatial Power Emissions for Radar Altimeter Interference Analysis," National Telecommunications and Information Administration, Boulder. CO, Tech. Rep. 22-562, October 2022. [Online]. Available: https://its.ntia.gov/publications/details.aspx?pub=3289

[7] M. Pirrone, M. K. Forsyth, J. Bernhardt, D. Kuester, A. Sanders, D. McGillivray, and A. Wunderlich, "Atic: Automated testbed for interference testing in communication systems," in *MILCOM 2023 - 2023 IEEE Military Communications Conference (MILCOM)*, 2023, pp. 599–604.

[8] E. D. Nelson and D. A. McGillivray, "In-Situ Captures of AWS-1 LTE for Aeronautical Mobile Telemetry System Evaluation," National Telecommunications and Information Administration, Boulder. CO, Tech. Rep. 21-553, March 2021. [Online]. Available: https://its.ntia.gov/publications/details.aspx?pub=3262

[9] P. A. Parker, G. G. Vining, S. R. Wilson, J. L. S. III, and N. G. Johnson, "The prediction properties of classical and inverse regression for the simple linear calibration problem," *Journal of Quality Technology*, vol. 42, no. 4, pp. 332–347, 2010. [Online]. Available: https://doi.org/10.1080/00224065.2010.11917831

[10] Kang, Pilsang, Koo, Changhoi, and Roh, Hokyu, "Reversed inverse regression for the univariate linear calibration and its statistical properties derived using a new methodology," *Int. J. Metrol. Qual. Eng.*, vol. 8, p. 28, 2017. [Online]. Available: https://doi.org/10.1051/ijmqe/2017021

[11] H. Kibirige, "Locally-weighted regression," 2016. [Online]. Available: https://has2k1.github.io/scikit-misc/loess.html

[12] P. Virtanen, R. Gommers, T. E. Oliphant, M. Haberland, T. Reddy, D. Cournapeau, E. Burovski, P. Peterson, W. Weckesser, J. Bright, S. J. van der Walt, M. Brett, J. Wilson, K. J. Millman, N. Mayorov, A. R. J. Nelson, E. Jones, R. Kern, E. Larson, C. J. Carey, İ. Polat, Y. Feng, E. W. Moore, J. VanderPlas, D. Laxalde, J. Perktold, R. Cimrman, I. Henriksen, E. A. Quintero, C. R. Harris, A. M. Archibald, A. H. Ribeiro, F. Pedregosa, P. van Mulbregt, and SciPy 1.0 Contributors, "SciPy 1.0: Fundamental Algorithms for Scientific Computing in Python," *Nature Methods*, vol. 17, pp. 261–272, 2020.

[13] D. Kuester, A. Wunderlich, D. McGillivray, D. Gu, and A. Puls, "Blind measurement of receiver system noise," *IEEE Transactions on Microwave Theory and Techniques*, no. 68, 2020-06-05 2020.